

Article

Research on the Influence of Euro VI Diesel Engine Assembly Consistency on NO_x Emissions

Wei Yan ¹, Tengyao Dou ¹, Jinbo Wang ², Na Mei ¹ and Guoxiang Li ^{2,*}

¹ School of Energy and Power Engineering, Shandong University, Jinan 250061, China; yanwei@sdu.edu.cn (W.Y.); dtywork2020@163.com (T.D.); meina0017@163.com (N.M.)

² Weichai Holding Group Co., Ltd., Weifang 262100, China; wjb_110@126.com

* Correspondence: liguox@sdu.edu.cn

Received: 30 June 2020; Accepted: 20 August 2020; Published: 13 October 2020



Abstract: The assembly consistency of a diesel engine will affect its nitrogen oxides (NO_x) emission variation. In order to improve the NO_x emissions of diesel engines, a study was carried out based on the assembly tolerance variation of the diesel engine's combustion system. Firstly, a diesel engine which meets the Euro VI standards together with the experimental data is obtained. The mesh model and combustion model of the engine combustion system are built in the Converge software (version 2.4, Tecplot, Bellevue, DC, USA), and the experimental data is used to calibrate the combustion model obtained in the Converge software. Then, the four-factor and three-level orthogonal simulation experiments are carried out on the dimension parameters that include nozzle extension height, throat diameter, shrinkage diameter and combustion chamber depth. Through mathematical analysis on the experimental data, the results show that the variation of nozzle extension height and combustion chamber depth have a strong influence on NO_x emission results, and the variation of combustion chamber diameter also has a weak influence on NO_x production. According to the regression model obtained from the analysis, there is a quadratic function relating the nozzle extension height and NO_x emissions and the amount of NO_x increases with increasing nozzle extension height. The relationship between emission performance and size parameters is complex. In the selected size range, the influence of the variation of the chamber diameter on NO_x is linear. The variation of the chamber depth also has an effect on NO_x production, and the simulation results vary with the change of assembly tolerance variation. Thus, in the engine assembly process, it is necessary to strictly control the nozzle extension height and combustion chamber depth. The research results are useful to improve the NO_x emission of diesel engine and provide a basis for the control strategy of selective catalytic reduction (SCR) devices.

Keywords: assembly consistency; NO_x emissions; diesel engine; numerical simulation

1. Introduction

Due to the high energy density and their wide range of power output, diesel engines are widely used in various fields such as agriculture, industry, engineering, transportation and so on. However, the widespread use of diesel engine causes serious environmental pollution. To protect the environment, many countries in the world have introduced strict regulations to limit emissions [1]. The emission performance of diesel engines is affected by many parameters, such as combustion chamber geometry [2], mixture formation, EGR rate, thermal condition, fuel composition and so on.

Because the combustion system plays an important role, many scholars have studied the relationship between emission performance and combustion systems based on bench tests and numerical simulations. Using an experiment method, Vedharaj [3] compared the effects of three kinds of combustion chambers—trapezoidal combustion chamber (TRCC), toroidal combustion chamber

(TCC) and hemispherical combustion chamber (HCC)—on the emissions of a stationary diesel engine. The results indicated that NO_x emissions remained unchanged and the CO and soot emissions were reduced with a reasonable combustion chamber design. Jesús Benajes [4] studied the effect of combustion chamber geometry on the reactivity of a high load reactivity-controlled compression ignition engine (RCCI). The results showed that the three types of combustors could reduce NO_x and soot emissions under low load conditions. Seung [5] reduced the compression ratio by changing the shape of the combustion chamber and carried out experiments with a two-stage injection strategy. The results showed that this method could significantly reduce NO_x emissions and improve engine performance. Since numerical calculations can effectively save time and cost, AVL fire, KIVA-3V and Converge have been widely used for combustion calculation. Jesús Benajes [6] and Hu [7] calibrated the KIVA-3V combustion model according to the test data. Under the condition of determining the peak pressure and emission value, the shape of combustion chamber and the design of nozzle were studied and the results showed that the efficiency of diesel engine could be improved by improving the size parameters of diesel engine. Liu et al. [8], Khan et al. [9] and Tay et al. [10] used simulation software to optimize the performance of diesel engine under different fuel injection parameters and combustion chamber shape and obtained the optimal parameter combination under different loads. The above research results and methods are of great significance for the analysis of the relationship between the combustion system and diesel performance. However, there are few studies focusing on the influence of dimensional tolerance caused by assembly consistency on diesel performance. In the Euro IV and Euro V regulations, the emission limits of nitrogen oxides (NO_x) are 250 mg/km and 180 mg/km respectively, but in the Euro VI stage, the emission limit is 60 mg/km, decreasing by 66.7% compared with Euro V. Thus it is very important to control the variation of NO_x emissions caused by dimensional tolerance in the Europe VI stage. Since the dimensional tolerance is less than 0.1 mm, it is more effective to carry out the research by using the numerical simulation methods than the bench experiment methods. In this paper, a diesel engine which meets the Euro VI standards is taken as the research object. The mesh model and combustion model are built in the Converge software and calibrated by the experimental data. Then, orthogonal simulation experiments are used to study the influence of parameters, including nozzle extension height, throat diameter, shrinkage diameter and chamber depth, on the performance consistency of NO_x emissions. By using mathematical analysis, the relationship between combustion system size and NO_x emission is obtained. The research results are useful to improve the NO_x emission of diesel engine and provide a basis for the control strategy of selective catalytic reduction (SCR) devices.

2. Calibration of Combustion Model

2.1. Experimental Setup

The main parameters of the engine and the instrumentation used in experiment are shown in Tables 1 and 2.

The concentrations of NO_x, HC, CO and O₂ are measured with a MEXA-7500DEGR gas analyzer (HORIBA, Kyoto, Japan). The fuel consumption is measured with AVL 735 fuel consumption meter. The other particles in exhaust flow are measured with AVL 472 particle analyzer and FTUV ammonia leakage analyzer (Environmental Technology Co., Ltd., Puvasi, France) respectively. The AVL HT460 dynamometer can measure crank speed and mechanical torque.

2.2. Physical Model

Before CFD analysis of the diesel engine, a grid model was built. The three-dimensional mesh model of combustion chamber including intake and exhaust ports, cylinder liners and piston upper surfaces was defined. According to the solution requirements of the Converge software, the maximum size of the surface grid was 3 mm, and the minimum size was 1 mm to simulate the complete working cycle of the

diesel engine. Because of the small volume of the injector and the complexity of meshing, the parameters of the injector were set by the injection model in Converge. The model is shown in Figure 1.

Table 1. Main parameters of the diesel engine.

| Parameters of Engine | Valve |
|---------------------------------|---|
| Engine type | In line six cylinder, electronically controlled high pressure common rail |
| Bore diameter (mm) | 108 |
| Stroke (mm) | 137 |
| Connecting rod length (mm) | 209.7 |
| Clearance height (mm) | 1.71 |
| Compression ratio | 18 |
| Maximum valve lift (mm) | 11.00475 |
| Nozzle diameter (mm) | 0.183 |
| Rated Speed (r/min) | 2200 |
| Rated Power (kW) | 162 |
| Rated Fuel consumption (g/kW·h) | 219.9 |

Table 2. Main instrumentation of the experiments.

| Instrumentation | Type |
|--------------------------|-----------------|
| Dynamometer | AVL HT460/STARS |
| Fuel consumption meter | AVL 7351CST |
| Filter-type smoke meter | AVL 415SG002 |
| Opacity smoke meter | AVL 4390G004 |
| Particle analyzer | AVL 472 |
| Gas analyzer | MEXA-7500DEGR |
| Ammonia leakage analyzer | FTUV |

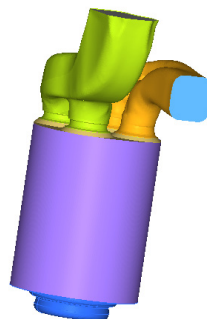


Figure 1. Grid model of diesel engine combustion chamber.

When setting up in Converge [11], a series of calculation models should be determined, such as turbulence model, atomization model, combustion model, emission model and so on. According to the actual working condition of diesel engine and relevant literature, each calculation model [11] is set as in Table 3:

Table 3. Physical model.

| Physical Model | Specific Model |
|------------------------|---------------------|
| Turbulence model | RNG k-epsilon |
| Heat transfer model | Han and Reitz model |
| Atomization model | KH-RT |
| Spray-wall interaction | Wall film |
| Fuel impact model | NTC |
| Combustion model | SAGE |
| NOx emission model | Extend Zel'dovich |

2.2.1. Turbulence Model

Considering the flow process of the combustion chamber, RNG k-epsilon model [12] is selected in the calculation. Compared with the standard k-epsilon model, the RNG k-epsilon model modifies the turbulent viscosity and adds the turbulent dissipation. The model equations are as follows:

$$\frac{\partial \rho k}{\partial t} + \frac{\partial \rho u_i k}{\partial x_i} = \tau_{ij} \frac{\partial u_i}{\partial x_j} + \frac{\partial}{\partial x_j} \left(\frac{\mu}{Pr_k} \frac{\partial k}{\partial x_j} \right) - \rho \epsilon + S_s \quad (1)$$

$$\frac{\partial \rho \epsilon}{\partial t} + \frac{\partial (\rho u_i \epsilon)}{\partial x_i} = \frac{\partial}{\partial x_j} \left(\frac{\mu}{Pr_\epsilon} \frac{\partial \epsilon}{\partial x_j} \right) + c_{\epsilon 3} \rho \epsilon \frac{\partial u_i}{\partial x_i} + \left(c_{\epsilon 1} \frac{\partial u_i}{\partial x_i} \tau_{ij} - c_{\epsilon 2} \rho \epsilon + c_s S_s \right) \frac{\epsilon}{k} - \rho R \quad (2)$$

$$R = \frac{C_\mu \eta^3 (1 - \frac{\eta}{\eta_0})}{(1 + \beta \eta^3)} \frac{\epsilon^2}{k} \quad (3)$$

In the equations above, C_μ is 0.0845, $c_{\epsilon 1}$ is 1.42, $c_{\epsilon 2}$ is 1.68, $c_{\epsilon 3}$ is -1.0 ; η_0 is 4.38; β is 0.012; Reciprocal TKE Prandtl is 1.39; Reciprocal TKE ϵ Prandtl is 1.39.

2.2.2. Atomization Model

The KH-RT model [13] is adopted to simulate the atomization process. The KH model simulates the first splitting of fuel droplets and the RT model simulates the process of the second crushing of fuel droplets. The governing equation of the crushing length of the liquid core in the KH model is as follows:

$$L_b = C_{bl} \sqrt{\frac{\rho_l}{\rho_g}} d_0 \quad (4)$$

When the droplet is broken for the second time, the droplet radius change rate is as follows:

$$\frac{dr}{dt} = \frac{r - r_c}{\tau} \quad (5)$$

2.2.3. Combustion Model

Converge software contains a variety of combustion models, among which SAGE model [14] simulates the chemical reaction in the combustion process by using the input chemkin format file containing detailed chemical reaction mechanism and chemical reaction kinetics.

2.2.4. Emission Model

The main emissions of diesel engine are NOx and soot. To predict NOx emission, Zel'Dovich's NOx model [15] was adopted. 90% of the NOx generated by the diesel engine is NO. According to the chemical reaction equation, the formation rate of NO is as follows:

$$\frac{d[N]}{dt} = k_{R1,f}[O][N_2] - k_{R1,r}[NO][N] - k_{R2,f}[N][O_2] + k_{R2,r}[NO][O] - k_{R3,f}[N][OH] + k_{R3,r}[NO][H] \quad (6)$$

Assuming that the chemical reaction of N is in a steady state and its change rate is a fixed value, the formula for the formation rate of NO is as follows:

$$\frac{d[N]}{dt} = k_{R1,f}[O][N_2] - k_{R1,r}[NO][N] - k_{R2,f}[N][O_2] + k_{R2,r}[NO][O] - k_{R3,f}[N][OH] + k_{R3,r}[NO][H] \quad (7)$$

Assuming that the formation rate of N is 0, the formula of NO formation rate is as follows:

$$\frac{d[NO]}{dt} = 2k_{R1,f}[O][N_2] \frac{1 - [NO]^2 / (k[O_2][N_2])}{1 + k_{R1,r}[NO] / (k_{R2,f}[O_2] + k_{R3,f}[OH])} \quad (8)$$

The grid model is imported into the Converge software, and the physical model in the Table 3 is selected. The initial parameters are obtained by experiments.

2.3. Result Analysis and Reliability Verification

2.3.1. Model Reliability Verification

The operating point is Non-road Steady Cycle (NRSC). In this case, the parameters of the diesel engine are as follows: rated speed of 2200 r/min, power of 162 kW, fuel consumption of 219.9 g/kW·h, etc. Based on this condition, comparing the experimental results with the simulation results, the NOx emission obtained from the experiment is 8.15 g/kW·h, and the simulated NOx emission is 8.06 g/kW·h, with an error of 1.1%; The error of fuel consumption is 1.1%. The maximum burst pressure is 16.7 MPa, meeting the requirements of less than 17.5 MPa. The error between the simulation results and the experiment is within the acceptable range, which shows that the calculation model is reliable and can be further studied.

2.3.2. Analysis of Calculation Results

As shown in Figure 2a, when entering the fast combustion period, the pressure in the cylinder increases rapidly and reaches the peak value. From the end of the fast burning period to the end of combustion, the pressure decreases gradually. The highest value of cylinder pressure is about 6 crank angle (CA) after top dead center (ATDC), which is 16.7 MPa.

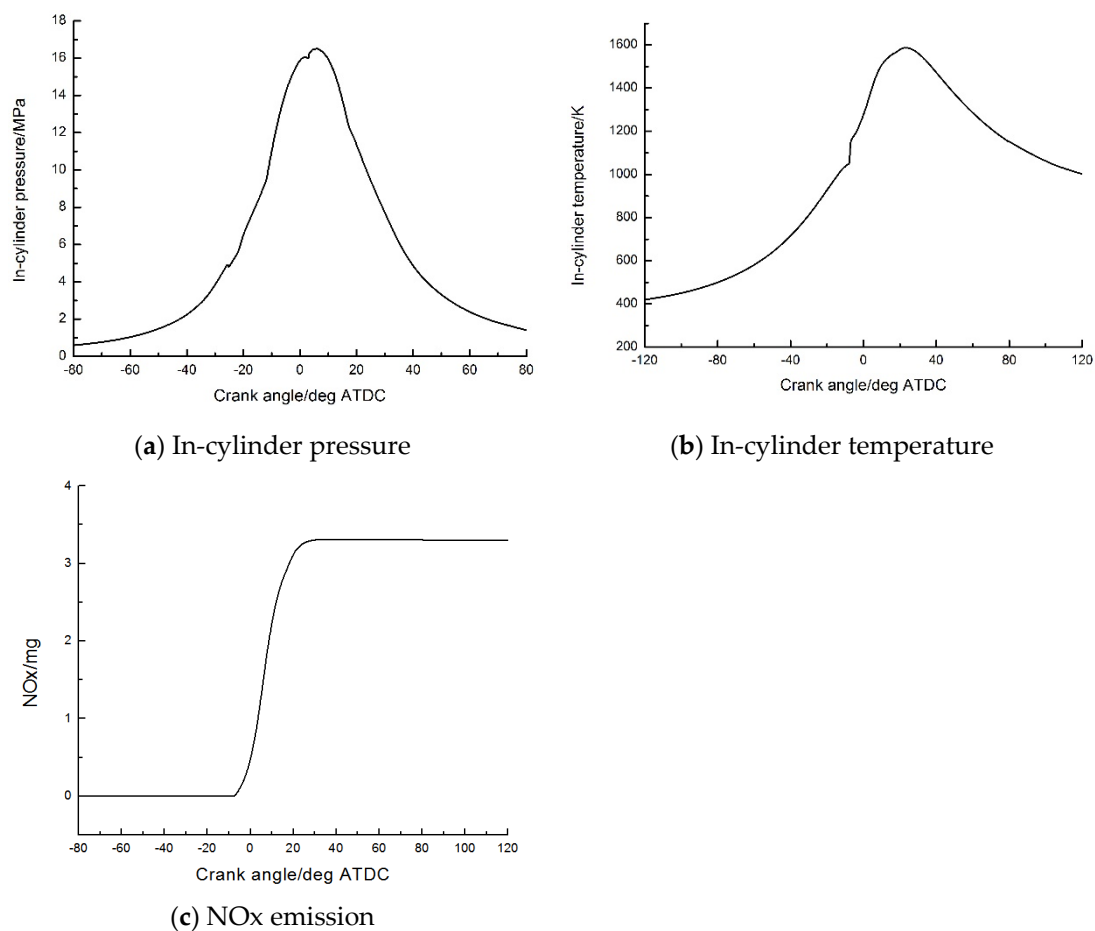


Figure 2. Pressure temperature NOx emission results.

Figure 3b shows the temperature curve in the cylinder. The temperature change trend in the cylinder is basically the same as that of pressure, which rises rapidly first and then decreases.

According to Figure 3d,g, in the initial stage of combustion, the temperature near the injection position is significantly higher than the surrounding temperature, indicating the combustion starts near the injection nozzle.

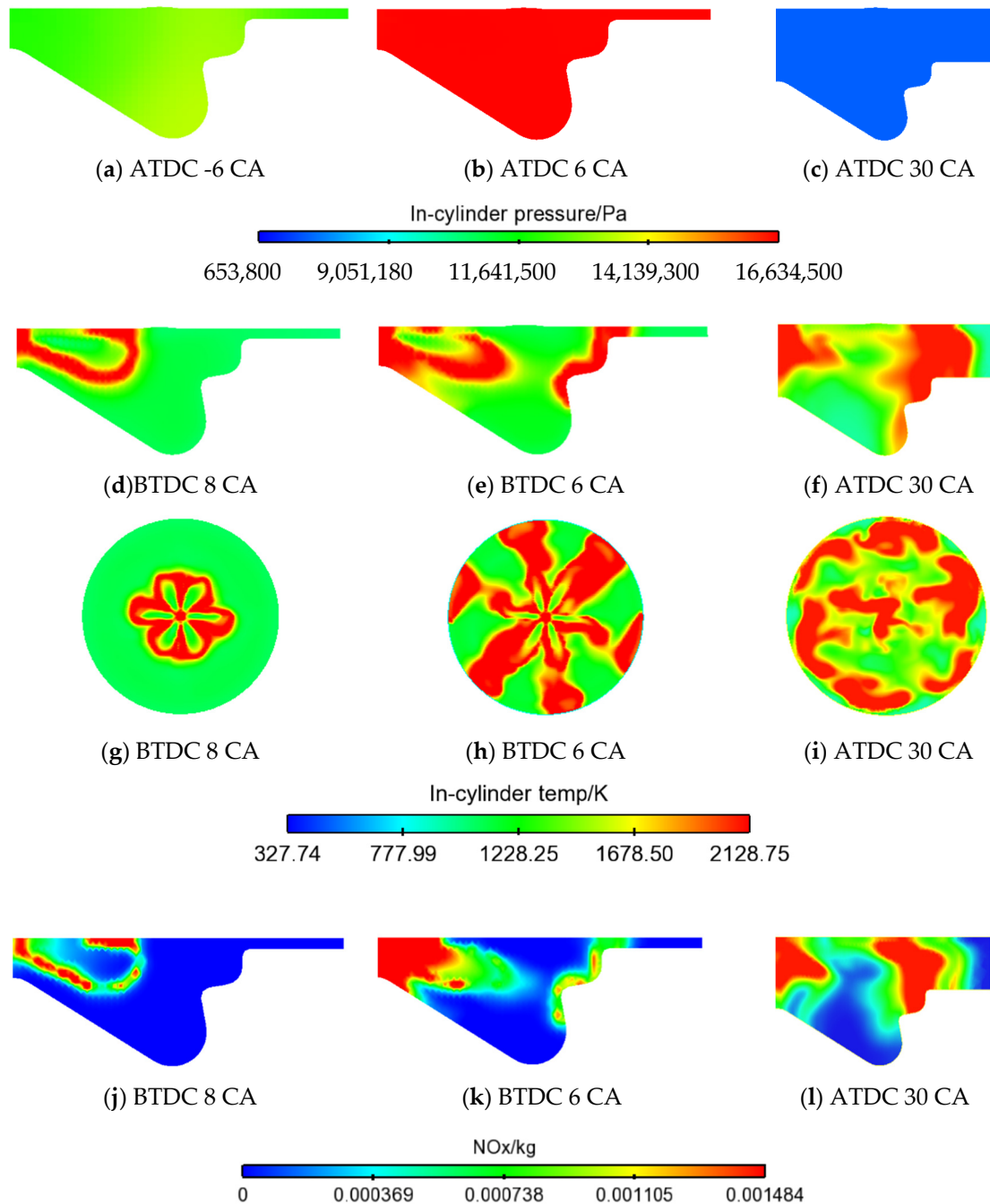


Figure 3. Pressure temperature NOx emission distribution.

The ignition position is at the edge of the fuel-air mixing position. As shown in Figure 3e,h, the flame diffusion direction is the same as that in the spray direction, and the fuel near the wall begins to burn. Then the flame further diffuses to the clearance and the bottom of chamber. It can be seen from the Figure 3i that the temperature distribution in the combustion chamber is relatively uniform, and the fuel is almost completely burned at this time.

Figure 2c shows the curve of NOx produced. At the beginning of combustion, the pressure and temperature in the cylinder rise rapidly due to the rapid combustion of mixture in the cylinder. And there is enough oxygen near the high temperature flame to produce a large amount of NOx in the cylinder. According to Figure 3d,j, the location of NOx enrichment is the same as that of the high temperature in the cylinder, and the same rule exists in the distribution of NOx in Figure 3e,k,f,l. With the further development of combustion in the cylinder, the oxygen content in the cylinder is significantly reduced due to the combustion process, which leads to the instantaneous NOx production is significantly reduced. The final NOx production in the cylinder is 3.33 mg.

3. Effect of Assembly Consistency on NOx Emission

3.1. Orthogonal Experimental Design

The quality and concentration distribution of the fuel-air mixture in the combustion chamber have an important influence on the diffusion combustion of the diesel engine, thus affecting the dynamic performance and NOx emission. While the mixture quality of fuel-air is affected by the shape of combustion chamber. The geometric dimension of combustion chamber mainly depends on the following parameters: throat diameter, shrinkage diameter and combustion chamber depth as shown in Figure 4.

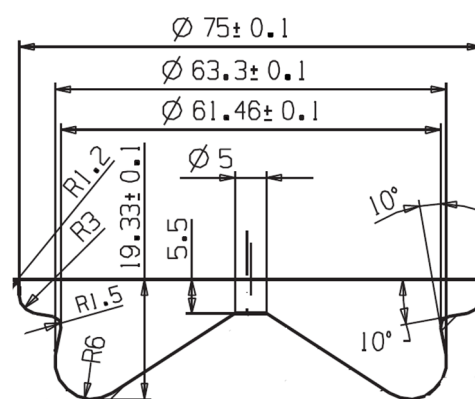


Figure 4. Chamber size parameters.

In the consideration of the piston deformation in the actual working state, the thermal mechanical coupling deformation is calculated. The results show that thermal expansion of the inside and outside diameter of the piston will be in equal proportion when it is working, so the original piston combustion chamber is used as the model for calculation in this paper.

Take three levels for each factor according to the dimensional tolerance specified in the product drawing. The orthogonal experiment design [16] is adopted to ensure the representative of the experiment. Table 4 shows the level of each factor, and Table 5 shows the orthogonal test list.

Table 4. Parameters of each dimensions.

| Factor Level | Nozzle Extension Height (mm) | Throat Diameter (mm) | Shrinkage Diameter (mm) | Chamber Depth (mm) |
|-----------------|---------------------------------|-------------------------|----------------------------|-----------------------|
| Level 1 | 0.77 | 74.9 | 61.36 | 19.23 |
| Level 2 | 1.02 | 75.0 | 61.46 | 19.33 |
| Level 3 | 1.52 | 75.1 | 61.56 | 19.43 |

Table 5. Orthogonal test.

| Factor NO. | Nozzle Extension Height (mm) | Throat Diameter (mm) | Shrinkage Diameter (mm) | Chamber Depth (mm) |
|---------------|---------------------------------|-------------------------|----------------------------|-----------------------|
| 1 | 0.77 | 74.9 | 61.36 | 19.23 |
| 2 | 0.77 | 75.0 | 61.46 | 19.33 |
| 3 | 0.77 | 75.1 | 61.56 | 19.43 |
| 4 | 1.02 | 74.9 | 61.46 | 19.43 |
| 5 | 1.02 | 75.0 | 61.56 | 19.23 |
| 6 | 1.02 | 75.1 | 61.36 | 19.33 |
| 7 | 1.52 | 74.9 | 61.56 | 19.33 |
| 8 | 1.52 | 75.0 | 61.36 | 19.43 |
| 9 | 1.52 | 75.1 | 61.46 | 19.23 |

3.2. Analysis of Experimental Results

The influence of each factor on NO_x emission is obtained by regression analysis, and the four independent variables of nozzle extension height, throat diameter, shrinkage diameter and chamber depth were recorded as a, b, c and d respectively. Table 6 shows the regression analysis results of NO_x.

Table 6. Regression analysis results.

| Model | R | R ² | R ² _{adj} | F | Sig |
|----------------|-------------|----------------|-------------------------------|--------|--------|
| Valve | 0.985 | 0.970 | 0.952 | 53.068 | 0.0003 |
| Model | Coefficient | | t | Sig | |
| constant | 30.077554 | | 2.191 | 0.080 | |
| a ² | −1.483293 | | −2.916 | 0.033 | |
| b ² | −0.005301 | | −2.173 | 0.082 | |
| abcd | 0.000052 | | 3.883 | 0.012 | |

The regression equation can be concluded as follows:

$$y_{\text{NO}_x} = 30.077554 - 1.483293a^2 - 0.005301b^2 + 0.000052ab \text{ cd} \quad (9)$$

Regression analysis and significance analysis show that sig < 0.05, indicating that the model was very significant. The determined coefficient of the model, namely the adjusted R-square value, is 0.952, indicating that the linear relationship between the dependent variable and the independent variable of the model is significant.

When the significance of the independent variable factors obtained from regression analysis is less than 0.05, it indicates that the independent variable is significant. It can be seen from the calculation results that the nozzle extension height has a significant impact on NO_x generation, and other factors also have an impact on emission. The influence of single factor on its performance is studied.

3.3. The Effect of Nozzle Extension Height Inconsistency on NO_x Emission

The different nozzle extension heights lead to the different positions of fuel spray and wall impact, the different degree of fuel-air mixing, and the different combustion efficiency. With the combustion model, at 30 CA ATDC, the temperature field distribution of different nozzle extending height is shown in the Figure 5. When the nozzle extends 0.77 mm, 1.02 mm, 1.52 mm respectively, the maximum average in-cylinder temperature is 1560 k, 1586 k, 1625 k accordingly. According to the reaction mechanism of NO_x [15], higher temperature promotes the formation of NO_x. Figure 6 is the curve of accumulated NO_x production in the cylinder caused by the variation of nozzle extension height. With different nozzle extension heights, the cumulative NO_x production in the cylinder changes significantly. When the height is 0.77, 1.02 and 1.52 mm, respectively, the NO_x production is 2.942, 3.331

and 3.804 mg, accordingly. The results indicate that the change trend of NO_x emission is consistent with the regression Equation (9) shown.

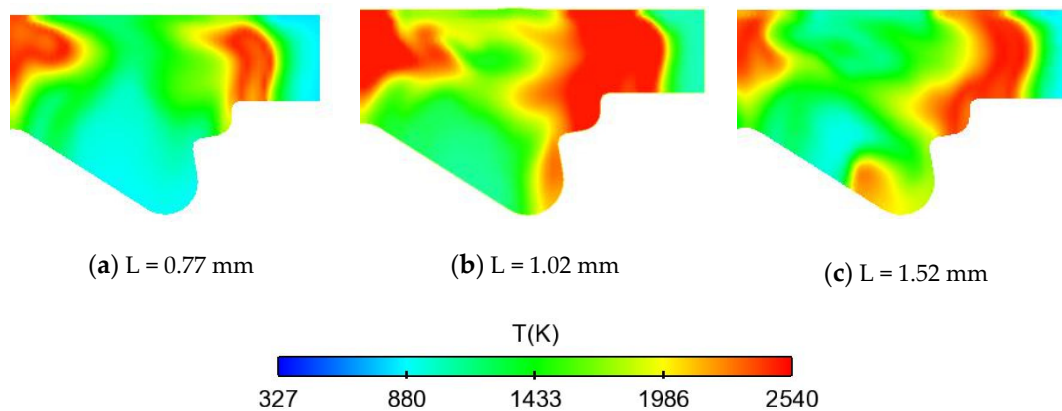


Figure 5. In-cylinder temperature distribution at 30 CA ATDC with different nozzle extension heights.

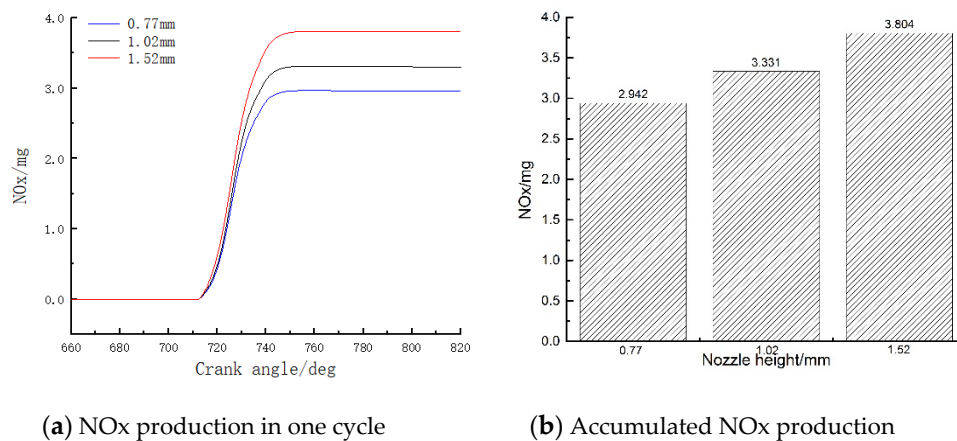


Figure 6. Accumulated NO_x production under different nozzle extension heights.

3.4. Effect of Internal Diameter Inconsistency on NO_x Emission

The variations of throat diameter and shrinkage diameter have an impact on the fuel-air mixture distribution, and then affect the combustion temperature and NO_x emission as mentioned in Section 3.3. According to the simulation results as shown in Figures 7 and 8, when the throat diameter is 74.9, 75.0 or 75.1 mm, respectively, the maximum average in-cylinder temperature is 1585, 1586 and 1560 K, accordingly. When the shrinkage diameter is 61.36, 61.46 or 61.56 mm respectively, the maximum average in-cylinder temperature is 1590, 1586 and 1594 K accordingly. This indicates that with the variation of chamber diameter, the accumulated amount of NO_x in the cylinder also changes in Figure 9. When the throat diameter is 74.9, 75.0 or 75.1 mm, respectively, the NO_x production is 3.334, 3.331 or 2.944 mg, accordingly; when the shrinkage diameter is 61.36, 61.46 or 61.56 mm, respectively, the NO_x production is 3.321, 3.331 or 3.346 mg, accordingly. According to the regression Equation (9), NO_x production decreases with the increase of throat diameter and increases with the increase of shrinkage diameter, which is consistent with the simulation results.

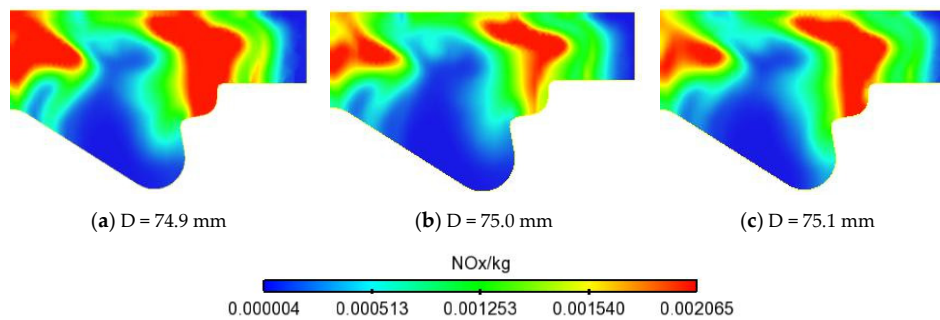


Figure 7. NOx distribution in 30 CA cylinder ATDC under different throat diameters.

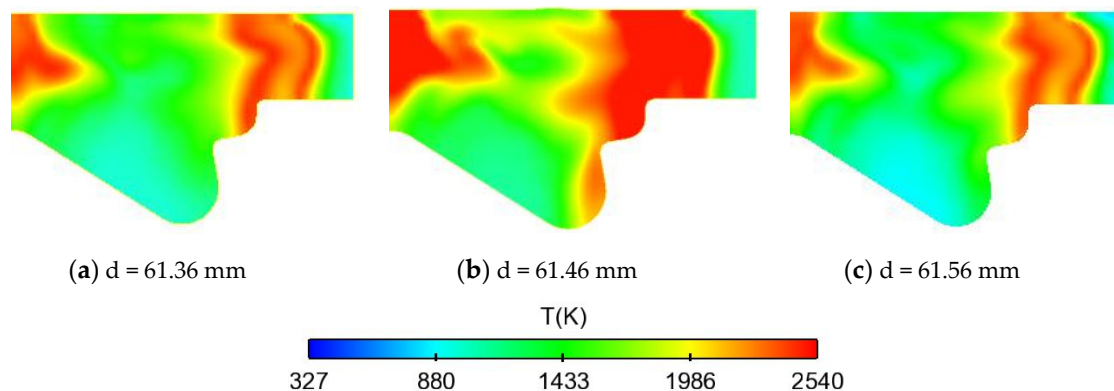


Figure 8. Temperature distribution in cylinder 30 CA ATDC with different shrinkage diameters.

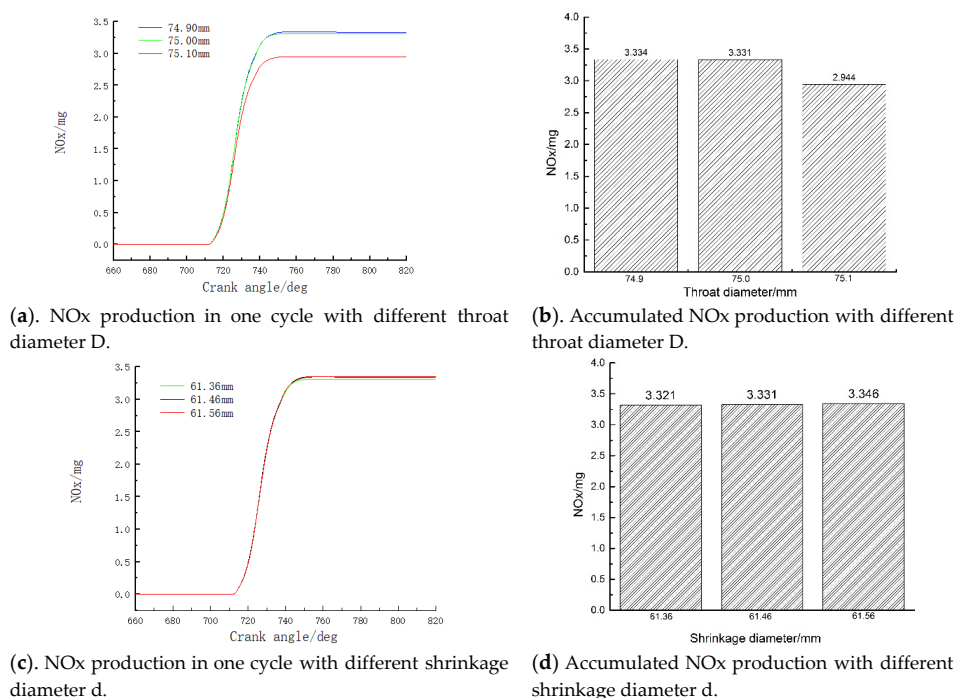


Figure 9. Accumulated NOx production in cylinder with different combustion chamber diameters.

3.5. The Effect of Combustion Chamber Depth Inconsistency on NOx Emission

According to the simulation results, it can be seen from the Figures 10 and 11 that the maximum average in-cylinder temperature and the accumulated NOx production change with different combustion chamber depths. When the combustion chamber depth is 19.23, 19.33 or 19.43 mm respectively, the maximum average in-cylinder temperature is 1590, 1586 or 1607 K and the NOx

production is 3.364, 3.331 or 3.523 mg, accordingly. In this case, the effect of different combustion chamber depths on NO_x emission is remarkable.

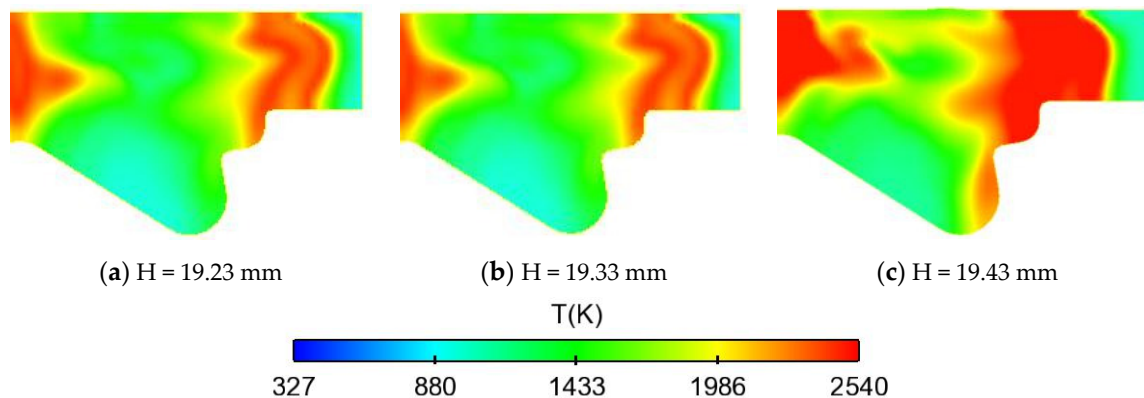


Figure 10. Temperature distribution in cylinder at 30CA ATDC at different combustion chamber depths.

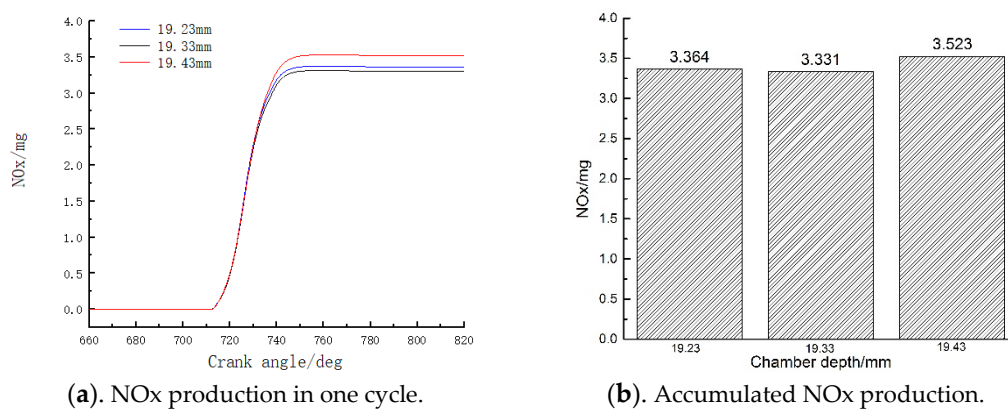


Figure 11. Accumulated NO_x production at different combustion chamber depths.

4. Conclusions

Based on the experimental data and Converge software, the relationship between the NO_x emission and size of diesel engine is studied. The main conclusions are as follows:

1. The combustion system grid model, and the combustion model are built in the converge software. The diesel engine bench test results are used to calibrate the combustion model.
2. The key dimension parameters (nozzle extension height, combustion chamber throat diameter, combustion chamber contraction diameter and combustion chamber depth) of the combustion system which affect combustion are selected for orthogonal testing. According to the regression equation of orthogonal test and the results of single factor test, there are associations between the NO_x emission and variation of parameters tolerance. The different parameters tolerance leads to different effects of fuel spray and fuel-air mixing in combustion chamber. Hence, different combustion efficiency results in varied combustion temperature and NO_x emission.
3. Based on the simulation results, the influence trend of each parameter is analyzed. In the range of 0.77–1.52 mm, increasing the nozzle extension height will significantly increase the Nox production, and the extended height should be controlled in the actual assembly process. There is a linear relationship between the diameter of the combustion chamber and the Nox emission. The depth of the combustion chamber also changes the Nox emission significantly. Then, the assembly tolerance of the engine must be strictly controlled.

Author Contributions: Conceptualization, methodology, and data curation, W.Y., G.L., and T.D.; Formal analysis, T.D.; Validation, W.Y. and T.D.; Resources and funding acquisition, J.W. and W.Y.; Writing—original draft preparation, T.D.; Writing—review and editing, W.Y., G.L. and N.M.; All authors have read and agreed to the published version of the manuscript.

Funding: This work was funded by the National Science and Technology Major Project of China under Grant No. 2018ZX04022001 and the Shandong province Key Research and Development Program of Grant No. 2017CXGC0603.

Conflicts of Interest: The authors declare no conflict of interest.

References

1. Mendoza-Villafuerte, P.; Suarez-Bertoa, R.; Giechaskiel, B.; Riccobono, F.; Bulgheroni, C.; Astorga, C.; Perujo, A. NO_x, NH₃, N₂O and PN real driving emissions from a Euro VI heavy-duty vehicle. Impact of regulatory on-road test conditions on emissions. *Sci. Total Environ.* **2017**, *609*, 546–555. [\[CrossRef\]](#)
2. Yan, B.; Wang, H.; Zheng, Z.; Qin, Y.; Yao, M. The effect of combustion chamber geometry on in-cylinder flow and combustion process in a stoichiometric operation natural gas engine with EGR. *Appl. Therm. Eng.* **2018**, *129*, 199–211. [\[CrossRef\]](#)
3. Vedharaj, S.; Vallinayagam, R.; Yang, W.M.; Saravanan, C.G.; Lee, P.S. Optimization of combustion bowl geometry for the operation of kapok biodiesel—Diesel blends in a stationary diesel engine. *Fuel* **2015**, *139*, 561–567. [\[CrossRef\]](#)
4. Benajes, J.; Pastor, J.V.; García, A.; Monsalve-Serrano, J. An experimental investigation on the influence of piston bowl geometry on RCCI performance and emissions in a heavy-duty engine. *Energy Convers. Manag.* **2015**, *103*, 1019–1030. [\[CrossRef\]](#)
5. Seung, H.Y.; Hyung, J.K.; Suhan, P. Study on Optimal Combustion Strategy to Improve Combustion Performance in a Single-Cylinder PCCI Diesel Engine with Different Combustion Chamber Geometry. *Appl. Therm. Eng.* **2018**, *144*, 1081–1090.
6. Benajes, J.V.; Novella, R.; Pastor, J.M.; Hernández-López, A.; Kokjohn, S.L. Computational optimization of the combustion system of a heavy duty direct injection diesel engine operating with dimethyl-ether. *Fuel* **2018**, *218*, 127–139. [\[CrossRef\]](#)
7. Hu, N.; Zhou, P.; Yang, J. Reducing emissions by optimising the fuel injector match with the combustion chamber geometry for a marine medium-speed diesel engine. *Transp. Res. Part D Transp. Environ.* **2017**, *53*, 1–16. [\[CrossRef\]](#)
8. Liu, J.; Wang, J.; Zhao, H. Optimization of the injection parameters and combustion chamber geometries of a diesel/natural gas RCCI engine. *Energy* **2018**, *164*, 837–852. [\[CrossRef\]](#)
9. Khan, S.; Panua, R.; Bose, P.K. Combined effects of piston bowl geometry and spray pattern on mixing, combustion and emissions of a diesel engine: A numerical approach. *Fuel* **2018**, *225*, 203–217. [\[CrossRef\]](#)
10. Tay, K.L.; Yang, W.; Zhao, F.; Yu, W.; Mohan, B. Numerical investigation on the combined effects of varying piston bowl geometries and ramp injection rate-shapes on the combustion characteristics of a kerosene-diesel fueled direct injection compression ignition engine. *Energy Convers. Manag.* **2017**, *136*, 1–10. [\[CrossRef\]](#)
11. *Converge Studio Manual*; Convergent Science, Inc.: Madison, WI, USA, 2016.
12. Yakhot, V.; Orszag, S.A.; Panda, R. Computational test of the renormalization group theory of turbulence. *J. Sci. Comput.* **1988**, *3*, 139–147. [\[CrossRef\]](#)
13. Senecal, P.K.; Richards, K.J.; Pomraning, E.; Yang, T.; Dai, M.Z.; McDavid, R.M.; Patterson, M.A.; Hou, S.; Shethaji, T. A New Parallel Cut-Cell Cartesian CFD Code for Rapid Grid Generation Applied to In-Cylinder Diesel Engine Simulations. *SAE Tech. Pap. Ser.* **2007**. [\[CrossRef\]](#)
14. Senecal, P.K.; Pomraning, E.; Richards, K.J.; Briggs, T.E.; Choi, C.Y.; McDavid, R.M.; Patterson, M.A. Multi-Dimensional Modeling of Direct-Injection Diesel Spray Liquid Length and Flame Lift-off Length using CFD and Parallel Detailed Chemistry. *SAE Tech. Pap. Ser.* **2003**. [\[CrossRef\]](#)
15. Heywood, J.B. *Internal Combustion Engine Fundamentals*; McGraw Hill, Inc.: New York, NY, USA, 1988.
16. Wenqing, L. *Design of Experiments*; Tsinghua University Press: Beijing, China, 2005.

